LAWRENCE
LIVERMORE
NATIONAL
LABORATORY

LLNL-JRNL-446472

YEAST METABOLIC FLUX MEASUREMENT BY ACCELERATOR MASS SPECTROMETRY

B. J. Stewart, A. Navid, K. Turteltaub, G. Bench

August 2, 2010

Analytical Chemistry

Disclaimer

Release Number: LLNL-JRNL-446472

YEAST METABOLIC FLUX MEASUREMENT BY ACCELERATOR MASS SPECTROMETRY

Benjamin J. Stewart, Ali Navid, Kenneth W. Turteltaub, and Graham Bench

Lawrence Livermore National Laboratory, Center for Accelerator Mass Spectrometry

7000 East Avenue P.O. Box 808, L-397 Livermore, CA 94551

Email: Stewart66@llnl.gov

ABSTRACT

Metabolic flux, the flow of metabolites through cellular networks of enzymes, represents the dynamic productive output of cells. Improved understanding of metabolic fluxes within cells will enable targeted manipulation of cellular pathways of medical and industrial importance to a greater degree than is currently possible. Flux balance analysis (FBA) is a constraint-based approach to modeling metabolic fluxes, but its utility is limited by a lack of experimental measurements. We hypothesize that incorporation of experimentally measured fluxes as system constraints should significantly improve the overall accuracy of FBA. We applied a novel, two-tiered approach in the yeast *Saccharomyces cerevisiae* to measure nutrient consumption rates (extracellular fluxes) and targeted intracellular fluxes using a ^{14}C-labeled precursor with HPLC separation and flux quantitation by accelerator mass spectrometry (AMS). These experimental results provided global constraints for the yeast FBA model (extracellular fluxes) which reduced model uncertainty by approximately 25%, proving our hypothesis.

TITLE RUNNING "Metabolic flux measurement by accelerator mass spectrometry"

KEYWORDS Metabolic flux analysis, Flux balance analysis, Accelerator mass spectrometry, glutathione, glutamate, glutamine, yeast

Metabolism consists of many interconnected networks of genes, enzymes, and metabolites, which interact to regulate cell function. While the genetic complement of the cell dictates what metabolic processes are possible, the mere knowledge of the metabolic reactions that can occur is insufficient for a thorough understanding of a cell's metabolic state. It is important to understand both the structure and the output of these metabolic networks in order to more fully elucidate cell function and accurately predict cellular responses to various conditions. Two methods used to study metabolic fluxes are metabolic flux analysis (MFA) and flux balance analysis (FBA). MFA is an experimental method used to measure the time-dependent output of metabolic pathways [1-5], while FBA is a computational tool that models cellular metabolism based on the law of mass balance [6-12].

Computational models have been developed to improve understanding of cellular metabolic activity for a wide variety of organisms [11, 13-17], but these models are limited by a lack of sufficient experimental data to make the models reflect nature more accurately. Because FBA is a constraint-based approach for assessing a genotype's metabolic capabilities, implementation of any additional constraints (i.e. experimental results) will improve accuracy of FBA models' predictions. Two of the most important classes of constraints that can be placed on FBA models are "internal flux constraints" and "external flux constraints". The latter constraints ensure that import of nutrients and export of waste are set to experimentally measured values or capped to physiologically feasible levels. The former constraints ensure that the flux through each metabolic reaction has values that are biologically reasonable and in accord with experimental measurements. Unfortunately, the difficult task of measuring intracellular fluxes has meant that in the majority of developed FBA models the internal fluxes are not adequately constrained. This shortcoming can lead to predictions of futile internal cycles (see Figure 1) which have no physiological relevance. The ideal solutions to overcome this problem

would be to provide tighter constraints on the internal fluxes of the model as well as include thermodynamic limitations on metabolic reactions [18, 19].

The difficulty of directly measuring metabolic fluxes hinders the acquisition of data that would constrain and improve FBA models [20]. The primary methods currently in use for the measurement of metabolic fluxes are ^{13}C-NMR, ^{13}C-GC-MS and ^{13}C-LC-MS [5, 10, 21-24]. Typical ^{13}C tracer experiments do not measure true fluxes, but make use of isotopic labeling patterns of metabolic endpoints, which are then incorporated into computational models to allow calculation of fluxes [5, 22]. While powerful in assessing the overall metabolic state of the cells under consideration, current techniques using ^{13}C suffer from several limitations. Due to the relatively high natural abundance of ^{13}C, it is necessary to heavily label the precursor compound to be traced [22]. This makes it difficult or impossible in many cases to follow low-abundance metabolites, including the pool of free amino acids and many other intermediary metabolites [20]. In addition, MFA techniques generally require the use of a minimal medium with a single carbon source, as additional media nutrients can interfere with measurement techniques [22]. It may also be difficult to derive relevant information from such experiments because the addition of large quantities of a single labeled precursor can significantly alter normal metabolism. Thus, lack of sensitivity, requirement of metabolic and isotopic steady states, and restriction of media components are important limitations of current MFA techniques [1, 5, 22, 25, 26].

The application of novel experimental techniques with improved sensitivity could enable direct measurement of intracellular metabolic fluxes. Although MFA experiments are primarily performed using cells in metabolic and isotopic steady-states, a recent trend toward measuring isotopic and metabolic non-steady state cultures is emerging [4, 27, 28]. Whereas the steady-state experiments provide only isotope incorporation ratios for relatively high-abundance metabolic endpoints, it is possible to monitor true fluxes using isotopic-nonstationary cultures if a sufficiently sensitive isotope measurement technique is used. It has been suggested that more informative data could be obtained by measuring intracellular intermediate metabolites rather than biomass endpoints [28]. This intermediate

metabolite information is not readily obtained using ^{13}C-MFA techniques due to the difficulty of achieving an adequate level of labeling, and in the case of free amino acids because the metabolite pool is very small compared to the quantity of amino acids present in proteins. Yanagimachi, Stafford et al reported the use of a ^{14}C-labeled precursor to measure metabolic fluxes directly using HPLC coupled with radiometric detection [29], and thereby demonstrated the utility of using ^{14}C for measuring metabolic fluxes. However, radiometric detection does not provide the optimal sensitivity possible and still suffers from the need for the use of heavily labeled substrates at unnaturally high concentrations. This measurement problem can potentially be solved by using accelerator mass spectrometry (AMS), which offers a 10^6-fold gain in ^{14}C quantitation relative to decay counting [30].

Experiments have previously been performed using AMS to quantitatively trace ^{14}C-labeled drugs and nutrients in organisms and tissues [30-37]. The sensitivity and inherent quantitative nature of AMS measurements suggest that this technique could be a useful adjunct to more traditional MFA methods. We therefore sought to extend the utility of AMS to the measurement of intracellular metabolic fluxes. Experiments were performed using ^{14}C-labeled glutamine to directly measure metabolic fluxes in *Saccharomyces cerevisiae* grown in synthetic complete media (SCM), with glutathione as the metabolic endpoint. Glutathione is a ubiquitous, thiol-containing antioxidant with a well-characterized biosynthetic pathway, and is maintained at nearly constant intracellular levels during non-stressed conditions, making it an ideal test case for proof-of-principle experiments. Results demonstrate that the use of a targeted labeling approach allows the measurement of metabolite fluxes through a specific pathway using nCi (pmol) levels of ^{14}C-labeled tracer. Thus, AMS may be an effective complement to traditional metabolic flux measurement methods.

EXPERIMENTAL SECTION

Chemicals and Materials. Unless otherwise specified, all chemicals were obtained from Sigma Chemical Company (St. Louis, MO) and were of the highest purity available. Yeast *Saccharomyces*

cerevisiae strain S288C was obtained from the American Type Culture Collection (ATCC, Manassas, VA). Uniformly-labeled ^{14}C-Glutamine was purchased from Moravek Biochemicals (Brea, CA).

Cell growth conditions and experimental sampling. *Saccharomyces cerevisiae* strain S288C was grown in synthetic complete medium (SCM) supplemented with all 20 proteinogenic amino acids (Sigma yeast synthetic media supplement without uracil, 76 mg/L, Leucine at 380 mg/L) and uracil (80 mg/L). Cells were grown and maintained in log-growth phase at 30° C with shaking at 230 rpm in a Gyrotory Water Bath Shaker (New Brunswick Scientific) for at least 24 hours before labeling experiments were started. Yeast cells were grown in the presence of 0.1 nCi/mL ^{14}C glutamine (Gln), which corresponds to a ratio of 1 molecule labeled Gln per 250,000 unlabeled Gln molecules. Cell density was measured using a SpectraMax Plus 384 microplate spectrophotometer at 600 nm (Molecular Devices, Sunnyvale, CA). All experiments were performed in triplicate. Cells were grown in log-phase, with aliquots collected every 30 minutes. Two- 2 mL aliquots were collected, cells were pelleted by centrifugation for 3 minutes at 10,000 rpm at -9° C, and the media was collected and removed. Media was further purified by centrifugation at 14,000 rpm for 10 minutes to remove remaining intact cells. Cell pellets were washed twice with 1 mL ice-cold PBS, after which polar metabolites were extracted as described below, or cells were frozen at -20° C for later analysis. Duplicate cell and media aliquots were collected for each time point. Polar metabolites were extracted as reported by Villas-Boas et al [38]. Briefly, cell pellets were combined with 200 µL ice-cold chloroform, 100 µL methanol, and 100 µL of 3 mM PIPES-3 mM EDTA, pH 7.4, and vortexed for 45 minutes at -20° C. The upper, aqueous phase was collected in a fresh tube and stored at -20 C, and the organic phase was re-extracted with 100 µL methanol and 100 µL PIPES-EDTA. Extracts were spun at 14,000 rpm at -9° C for 10 minutes. Experiments showed greater than 90% recovery for Gln, Glu, and GSH using this technique (data not shown). For cell analysis by AMS, cell pellets were re-suspended in 200 µL of sterile water.

HPLC of amino acids and GSH. Amino acids in the polar metabolite extract were derivatized with ortho-phthalaldehyde and separated by reversed-phase HPLC essentially as described previously [39,

40], but using a 1:1 ratio of sample:ortho-phthalaldehyde-mercaptopropionic acid solution (Agilent Technologies, Santa Clara, CA). HPLC fractions were collected for AMS analysis using a Gilson fraction collector (Gilson, Middletown, WI). HPLC separations were performed on an Agilent 1100 instrument (Agilent Technologies) using an Agilent Eclipse Plus C18 5 μm 4.6 x 150 mm column at 30° C. The internal standard L-2-aminobutyric acid was added to each polar metabolite or media sample prior to HPLC analysis to a final concentration of 7.6 μg/mL. HPLC conditions were as follows: Flow rate, 1.5 mL/ min. Mobile phase A: 10 mM Potassium tetraborate tetrahydrate, 10 mM potassium phosphate, pH 8.15. Mobile phase B: 45% Methanol, 45% acetonitrile, 10% water. Column: Agilent C18, flow rate: 1.5 mL/ minute. Gradient: Time 0, 2% B; 4 minutes, 6% B; 4.20 minutes, 8% B; 9.50 minutes, 23% B; 12.00 minutes, 27.5% B; 12.50 minutes, 30% B; 20.00 minutes; 50% B; 20.10 minutes, 100% B; 22.00 minutes, 100% B; 22.1 minutes, 2% B; stop time: 25 minutes. Detection was accomplished using an Agilent 1100 fluorescence detector, with excitation at 340 nm and emission at 450 nm [40]. Analyte concentrations were calculated using peak area under the curves (AUC) and standard curves generated using authentic standards for each metabolite of interest.

Sample graphitization and analysis by accelerator mass spectrometry. Aliquots of cells, media, and polar metabolite extracts were converted to graphite and analyzed by AMS as previously described [31]. For AMS, the following sample volumes were used: HPLC fractions, 300 μL + 1 μL tributyrin carrier; Polar metabolite pool, 10 μL + 1 μL tributyrin; Media, 2 μL + 1 μL tributyrin; Cells, 2 μL + 1 μL tributyrin. Accelerator mass spectrometry results in fraction Modern $^{14}C/C$ were converted to amol ^{14}C based on the total C measured in each sample. All experiments were performed in triplicate. Error bars indicate standard error of the mean. GraphPad Prism 5 software was used to generate graphs (GraphPad Software, La Jolla, CA).

Constraining the yeast FBA model with experimental measurements. The iND750 model of metabolism in yeast [41], was augmented to allow for the import of all constituent amino acids in the SCM medium up to a value of 1 mM/gDW/hr. Flux variability analysis [6]was conducted on the

unconstrained model and the variability for each reaction was recorded. Using experimental measurements, the amino acid uptake rates were set and new series of flux variability analyses were conducted. The improvements in global flux variability of the system were quantified using the equation:

$$V_T = \frac{\sum_{i=1}^{N} \left(\frac{v_i^+ - v_i^-}{v_{oi}^+ - v_{oi}^-} \right)}{N}$$

Where V_T is the normalized measure of global flux variability, N is the number of reactions in the model, v_i^+ and v_i^- represent the lower boundary and upper boundaries for flux of reaction i, and o denotes the values for the unconstrained model.

RESULTS AND DISCUSSION

Basic growth parameters and ^{14}C Gln uptake. Yeast cells were in log-growth phase throughout the duration of the labeling experiments, as indicated by composite growth curves (Figure 2A). It is therefore possible to assume metabolic steady-state for these experiments, as required for flux balance analysis. Figures 2B and 2C show intracellular amino acid concentrations over time. It is unclear why concentrations of Glu increase over time. Previous publications have shown similar time-dependent changes in intracellular levels of Glu in *Saccharomyces cerevisiae* grown in batch cultures [42, 43]. Figure 2D shows the total cellular accumulation of ^{14}C due to uptake and metabolism of ^{14}C Gln for the duration of the experiments. The increase in ^{14}C in the intracellular polar metabolite pool is shown in Figure 2E.

Extracellular Fluxes. Media amino acids were taken up by yeast at different rates, as shown in Figures 3A and 3B. A slight depletion of the ^{14}C label was observed from the beginning of the labeling experiment to 3.5 hours. Amino acids and ^{14}C label were almost entirely depleted from the media after 18.5 hours (data not shown). Incorporation of the measured amino acid uptake rates (extracellular metabolic fluxes) into the yeast FBA model provided global metabolic constraints, thus reducing the

uncertainty present in the model (Figure 3C). In the absence of experimental constraints, metabolic fluxes in this model are predicted using algorithms that find mathematical solutions that may or may not be realizable in a biological system. Thus, the unconstrained model provides solutions that may include futile cycling or unrealistic flux values. In Figure 3C, this uncertainty inherent in the unconstrained model is arbitrarily set to "1" (y-axis). Incorporation of each of the measured amino acid consumption rates into the FBA model provides biological constraints that cumulatively reduce the uncertainty in the model by nearly 25%. Thus, measurement of extracellular metabolic fluxes and incorporation of these experimental results into the FBA model constrains the model at a global level.

Intracellular Metabolite Fluxes. The flow of ^{14}C label through the metabolic pathway beginning at extracellular Gln and proceeding to intracellular GSH is shown in Figure 4A. Specific metabolites in which the ^{14}C label was traced include Gln, Glu, and GSH. No appreciable amount of ^{14}C was detected in any of the other amino acids measured. While GSH is a relatively abundant, biologically important biomolecule in yeast, in log-phase growth, the vast majority of the free glutamate pool is used for protein synthesis. Because the fluxes from Gln to Glu and from Glu to GSH are small, and because Gln is readily taken up by yeast, this pathway was an ideal target for the measurement of metabolic fluxes using AMS. Figure 4B shows flux with respect to cell number, and Figure 4C shows the ^{14}C label normalized against the intracellular concentration of Gln, Glu, and GSH respectively. These results show that Gln and Glu reached isotopic steady state during the course of the experiment, while GSH failed to reach isotopic steady state within the 3.5 hour timeframe of this study. These experiments likewise failed to detect the efflux or leakage of any ^{14}C-labeled material from the cells for the duration of the experiments. The relatively low uptake rate of media amino acids contrasted with a very high uptake of media glucose (data not shown). The ability to trace the flow of ^{14}C through a relatively low-flux pathway in the presence of a large molar excess of glucose (approximately 100-fold compared to total Gln) and 19 other amino acids at concentrations similar to that of Gln, together with the low degree

of labeling of the Gln precursor (1 in 250,000 Gln molecules, or approximately 4 x 10^{-7}% of total media carbon) highlights the utility of AMS for the measurement of low-level metabolic fluxes.

CONCLUSIONS

We have demonstrated the utility of the direct measurement of intracellular metabolic fluxes by AMS as an adjunct to existing techniques for measuring extracellular metabolic fluxes in this proof-of-principle study. This novel, two-tiered approach provided global constraints for the *Saccharomyces cerevisiae* FBA model (external metabolite fluxes), as well as detailed flux information for a targeted metabolic pathway (intracellular fluxes). The application of extracellular flux data to the FBA model reduced model uncertainty by nearly 25%. The ability to reliably measure intracellular metabolite fluxes in cells will enable computational modeling of metabolism with greater accuracy and improved biological relevance.

While AMS is extremely powerful in monitoring the fate of a ^{14}C label, it is currently most effective in tracing the metabolic fate and kinetics of relatively few, low-abundance cellular metabolites. Our novel application of AMS has overcome some critical limitations of traditional MFA methods, and was able to directly measure intracellular metabolite fluxes using a low-level ^{14}C label in cells grown in complete media, beginning at isotopic non-steady-state and proceeding to approximate steady-state with respect to glutamine and glutamate. Further experiments using AMS to examine fluxes of critical intracellular intermediates, coupled with global flux measurement techniques, will significantly enhance our understanding of metabolism, leading to a greatly improved ability to manipulate metabolic pathways of interest. It is necessary to continue to improve techniques for measuring metabolic fluxes and increase the number of extracellular and intracellular metabolites that can be traced simultaneously. These improvements will enable the refinement and validation of computational models of metabolic networks, which can then be applied to solve important biological problems.

Release Number: LLNL-JRNL-446472

Acknowledgements

This work was performed under the auspices of the US Department of Energy by Lawrence Livermore National Laboratory under Contract No. DE-AC52-07NA27344 and was supported by the National Institutes of Health, National Center for Research Resources, Biomedical Technology Program (P41RR013461) and LLNL LDRD 09-ERI-002. LLNL release number: LLNL-JRNL-446472.

References

1. Schilling, C.H., et al., *Combining pathway analysis with flux balance analysis for the comprehensive study of metabolic systems.* Biotechnol Bioeng, 2000. **71**(4): p. 286-306.
2. Wiechert, W., *13C metabolic flux analysis.* Metab Eng, 2001. **3**(3): p. 195-206.
3. Fiaux, J., et al., *Metabolic-flux profiling of the yeasts Saccharomyces cerevisiae and Pichia stipitis.* Eukaryot Cell, 2003. **2**(1): p. 170-80.
4. Iwatani, S., Y. Yamada, and Y. Usuda, *Metabolic flux analysis in biotechnology processes.* Biotechnol Lett, 2008. **30**(5): p. 791-9.
5. Sauer, U., *Metabolic networks in motion: 13C-based flux analysis.* Mol Syst Biol, 2006. **2**: p. 62.
6. Mahadevan, R. and C.H. Schilling, *The effects of alternate optimal solutions in constraint-based genome-scale metabolic models.* Metab Eng, 2003. **5**(4): p. 264-76.
7. Reed, J.L. and B.O. Palsson, *Thirteen years of building constraint-based in silico models of Escherichia coli.* J Bacteriol, 2003. **185**(9): p. 2692-9.
8. Price, N.D., et al., *Genome-scale microbial in silico models: the constraints-based approach.* Trends Biotechnol, 2003. **21**(4): p. 162-9.
9. Orth, J.D., I. Thiele, and B.O. Palsson, *What is flux balance analysis?* Nat Biotechnol, 2010. **28**(3): p. 245-8.
10. Blank, L.M., L. Kuepfer, and U. Sauer, *Large-scale 13C-flux analysis reveals mechanistic principles of metabolic network robustness to null mutations in yeast.* Genome Biol, 2005. **6**(6): p. R49.
11. Cakir, T., et al., *Flux balance analysis of a genome-scale yeast model constrained by exometabolomic data allows metabolic system identification of genetically different strains.* Biotechnol Prog, 2007. **23**(2): p. 320-6.
12. Murabito, E., et al., *Capturing the essence of a metabolic network: a flux balance analysis approach.* J Theor Biol, 2009. **260**(3): p. 445-52.
13. Raghunathan, A., et al., *Constraint-based analysis of metabolic capacity of Salmonella typhimurium during host-pathogen interaction.* BMC Syst Biol, 2009. **3**: p. 38.
14. Navid, A. and E. Almaas, *Genome-scale reconstruction of the metabolic network in Yersinia pestis, strain 91001.* Mol Biosyst, 2009. **5**(4): p. 368-75.
15. Feist, A.M., et al., *A genome-scale metabolic reconstruction for Escherichia coli K-12 MG1655 that accounts for 1260 ORFs and thermodynamic information.* Mol Syst Biol, 2007. **3**: p. 121.
16. Nookaew, I., et al., *The genome-scale metabolic model iIN800 of Saccharomyces cerevisiae and its validation: a scaffold to query lipid metabolism.* BMC Syst Biol, 2008. **2**: p. 71.
17. Chavali, A.K., et al., *Systems analysis of metabolism in the pathogenic trypanosomatid Leishmania major.* Mol Syst Biol, 2008. **4**: p. 177.
18. Beard, D.A., S.D. Liang, and H. Qian, *Energy balance for analysis of complex metabolic networks.* Biophys J, 2002. **83**(1): p. 79-86.
19. Henry, C.S., L.J. Broadbelt, and V. Hatzimanikatis, *Thermodynamics-based metabolic flux analysis.* Biophys J, 2007. **92**(5): p. 1792-805.
20. Lee, J.M., E.P. Gianchandani, and J.A. Papin, *Flux balance analysis in the era of metabolomics.* Brief Bioinform, 2006. **7**(2): p. 140-50.
21. Yuan, Y., T. Hoon Yang, and E. Heinzle, *(13)C metabolic flux analysis for larger scale cultivation using gas chromatography-combustion-isotope ratio mass spectrometry.* Metab Eng, 2010.
22. Zamboni, N., et al., *(13)C-based metabolic flux analysis.* Nat Protoc, 2009. **4**(6): p. 878-92.
23. Costenoble, R., et al., *13C-Labeled metabolic flux analysis of a fed-batch culture of elutriated Saccharomyces cerevisiae.* FEMS Yeast Res, 2007. **7**(4): p. 511-26.
24. Metallo, C.M., J.L. Walther, and G. Stephanopoulos, *Evaluation of 13C isotopic tracers for metabolic flux analysis in mammalian cells.* J Biotechnol, 2009. **144**(3): p. 167-74.

25. Wiechert, W. and K. Noh, *From stationary to instationary metabolic flux analysis.* Adv Biochem Eng Biotechnol, 2005. **92**: p. 145-72.
26. Mo, M.L., B.O. Palsson, and M.J. Herrgard, *Connecting extracellular metabolomic measurements to intracellular flux states in yeast.* BMC Syst Biol, 2009. **3**: p. 37.
27. Noh, K., A. Wahl, and W. Wiechert, *Computational tools for isotopically instationary 13C labeling experiments under metabolic steady state conditions.* Metab Eng, 2006. **8**(6): p. 554-77.
28. Noh, K. and W. Wiechert, *Experimental design principles for isotopically instationary 13C labeling experiments.* Biotechnol Bioeng, 2006. **94**(2): p. 234-51.
29. Yanagimachi, K.S., et al., *Application of radiolabeled tracers to biocatalytic flux analysis.* Eur J Biochem, 2001. **268**(18): p. 4950-60.
30. Turteltaub, K.W. and J.S. Vogel, *Bioanalytical applications of accelerator mass spectrometry for pharmaceutical research.* Curr Pharm Des, 2000. **6**(10): p. 991-1007.
31. Brown, K., K.H. Dingley, and K.W. Turteltaub, *Accelerator mass spectrometry for biomedical research.* Methods Enzymol, 2005. **402**: p. 423-43.
32. Brown, K., E.M. Tompkins, and I.N. White, *Applications of accelerator mass spectrometry for pharmacological and toxicological research.* Mass Spectrom Rev, 2006. **25**(1): p. 127-45.
33. Lappin, G. and R.C. Garner, *The use of accelerator mass spectrometry to obtain early human ADME/PK data.* Expert Opin Drug Metab Toxicol, 2005. **1**(1): p. 23-31.
34. Links, J., et al., *Quantitative metabolism using AMS: Choosing a labeled precursor.* Nucl Instrum Methods Phys Res B, 2010. **268**(7-8): p. 1309-1312.
35. Vogel, J.S., *Accelerator mass spectrometry for quantitative in vivo tracing.* Biotechniques, 2005. **Suppl**: p. 25-9.
36. Vogel, J.S. and A.H. Love, *Quantitating isotopic molecular labels with accelerator mass spectrometry.* Methods Enzymol, 2005. **402**: p. 402-22.
37. White, I.N. and K. Brown, *Techniques: the application of accelerator mass spectrometry to pharmacology and toxicology.* Trends Pharmacol Sci, 2004. **25**(8): p. 442-7.
38. Villas-Boas, S.G., et al., *Global metabolite analysis of yeast: evaluation of sample preparation methods.* Yeast, 2005. **22**(14): p. 1155-69.
39. Hans, M.A., E. Heinzle, and C. Wittmann, *Quantification of intracellular amino acids in batch cultures of Saccharomyces cerevisiae.* Appl Microbiol Biotechnol, 2001. **56**(5-6): p. 776-9.
40. Kand'ar, R., et al., *Determination of reduced and oxidized glutathione in biological samples using liquid chromatography with fluorimetric detection.* J Pharm Biomed Anal, 2007. **43**(4): p. 1382-7.
41. Duarte, N.C., M.J. Herrgard, and B.O. Palsson, *Reconstruction and validation of Saccharomyces cerevisiae iND750, a fully compartmentalized genome-scale metabolic model.* Genome Res, 2004. **14**(7): p. 1298-309.
42. Hans, M.A., E. Heinzle, and C. Wittmann, *Free intracellular amino acid pools during autonomous oscillations in Saccharomyces cerevisiae.* Biotechnol Bioeng, 2003. **82**(2): p. 143-51.
43. Carter, B.L. and H.O. Halvorson, *Periodic changes in rate of amino acid uptake during yeast cell cycle.* J Cell Biol, 1973. **58**(2): p. 401-9.

Figures

Figure 1.

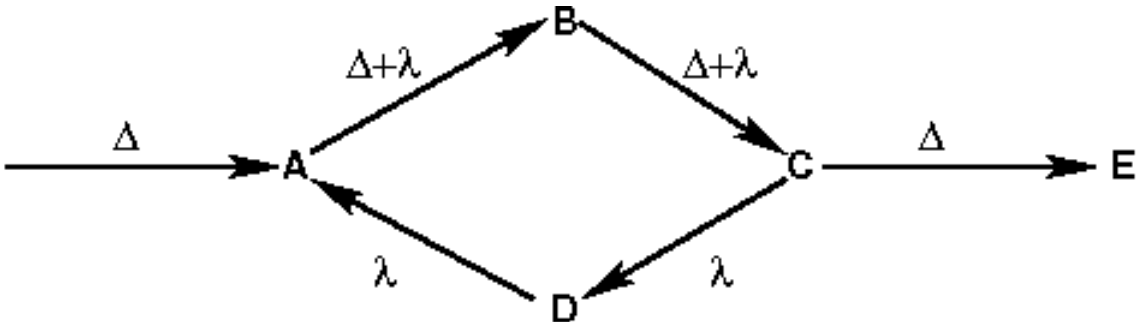

Figure 2.

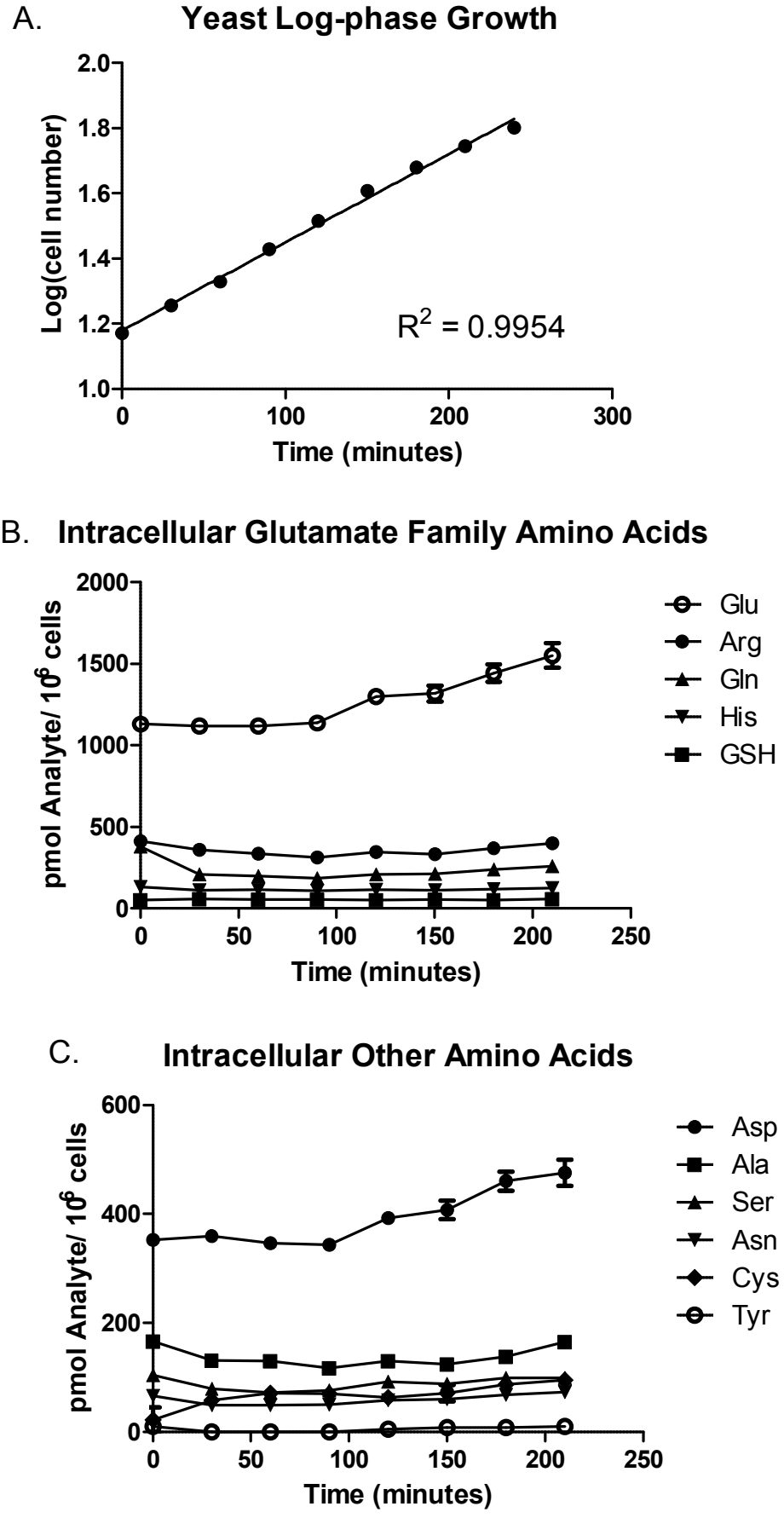
A.
Yeast Log-phase Growth
Log(cell number)
2.0
1.8
1.6
1.4
1.2
1.0
0
100
200
300
Time (minutes)
R2 = 0.9954
B.
Intracellular Glutamate Family Amino Acids
pmol Analyte/ 10^6 cells
2000
1500
1000
500
0
0
50
100
150
200
250
Time (minutes)
Glu
Arg
Gln
His
GSH
C.
Intracellular Other Amino Acids
pmol Analyte/ 10^6 cells
600
400
200
0
0
50
100
150
200
250
Time (minutes)
Asp
Ala
Ser
Asn
Cys
Tyr

D.

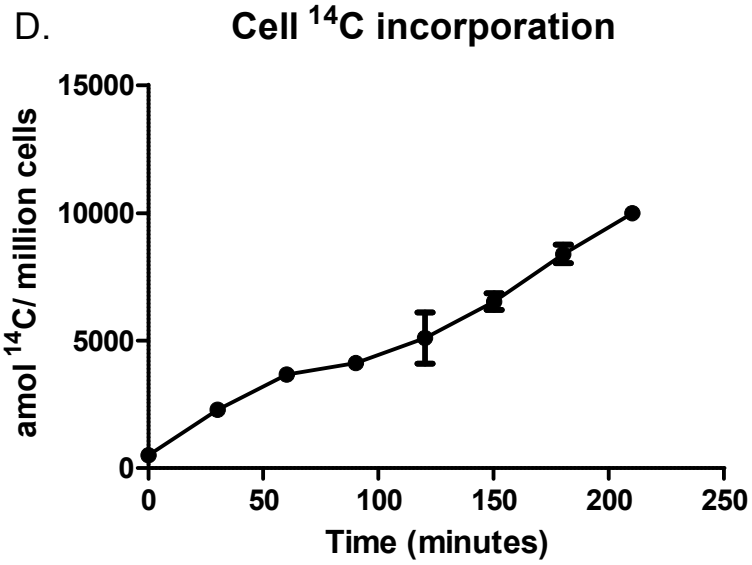
Cell 14C incorporation
amol 14C/ million cells
15000
10000
5000
0
0
50
100
150
200
250
Time (minutes)

E.

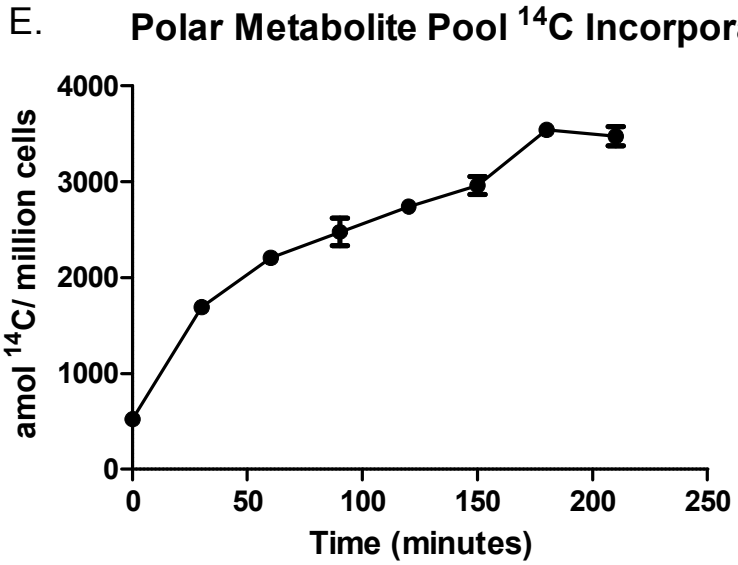
Polar Metabolite Pool 14C Incorporation
amol 14C/ million cells
4000
3000
2000
1000
0
0
50
100
150
200
250
Time (minutes)

Figure 3.

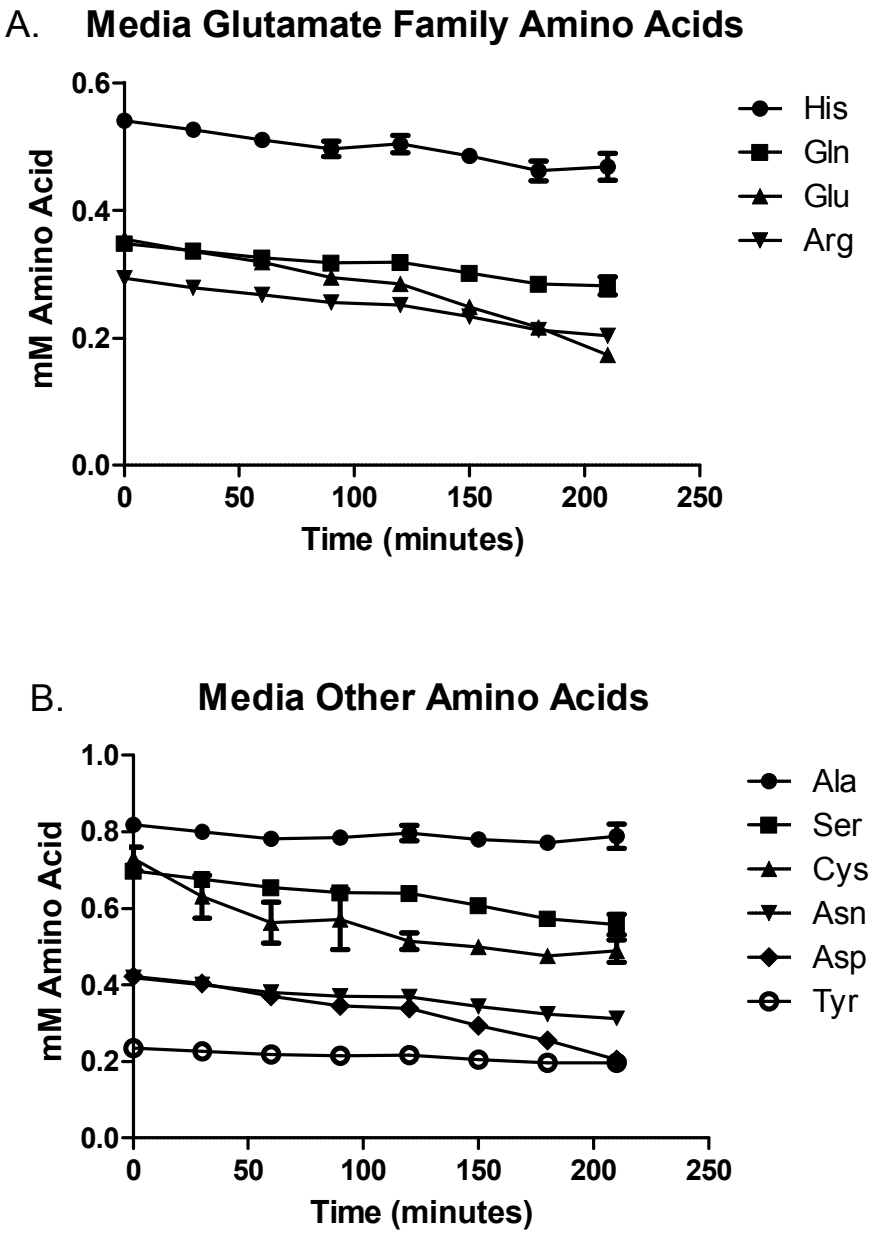
A.
Media Glutamate Family Amino Acids
mM Amino Acid
0.0
0.2
0.4
0.6
0
50
100
150
200
250
Time (minutes)
His
Gln
Glu
Arg
B.
Media Other Amino Acids
mM Amino Acid
0.0
0.2
0.4
0.6
0.8
1.0
0
50
100
150
200
250
Time (minutes)
Ala
Ser
Cys
Asn
Asp
Tyr

C. Yeast Model Constraint Using Extracellular Fluxes

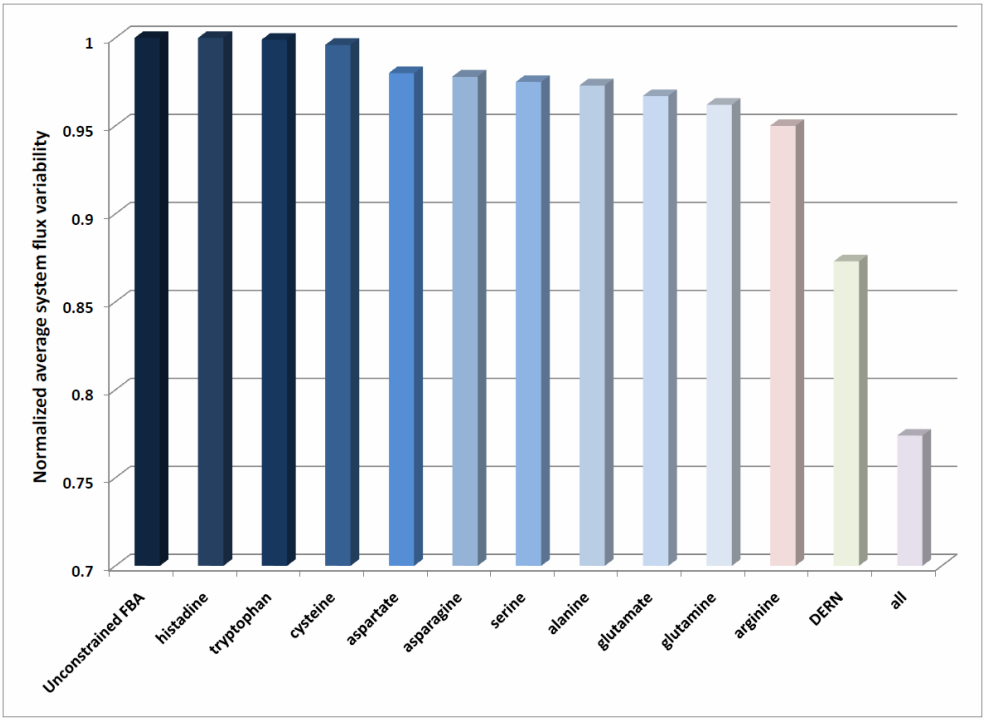

Figure 4.

A.

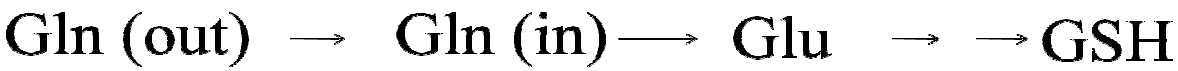

B. **Metabolite amol ^{14}C / 10^6 Cells**

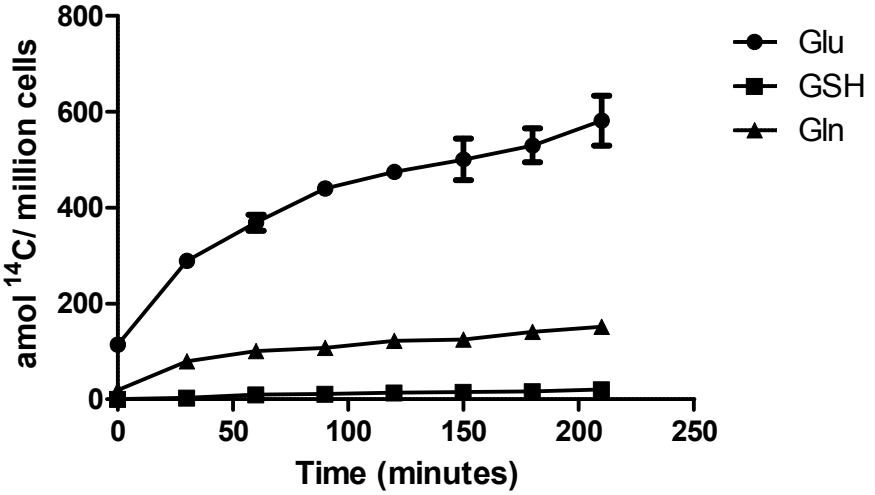

C. **amol ^{14}C per pmol Metabolite**

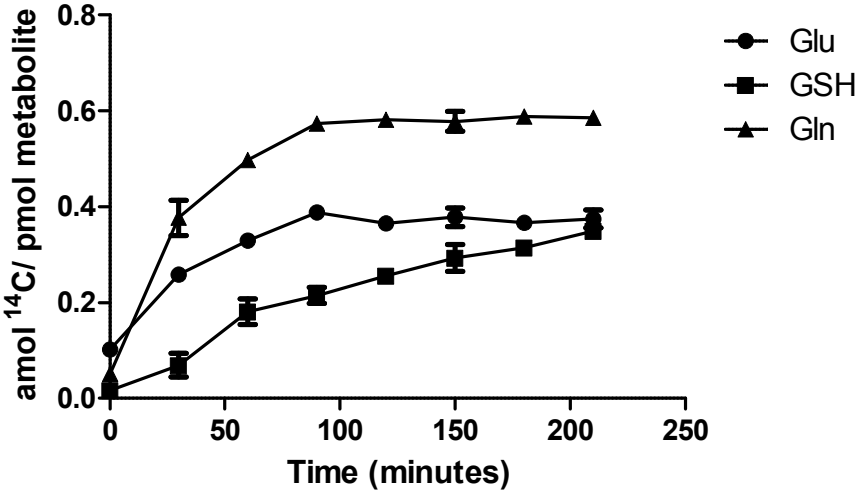

Figure Legends

Figure 1. An example of futile cycles in a metabolic network. In this example any value of λ will provide a reasonable mathematical solution to the flux analysis exercise. This problem can only be solved if either: a) thermodynamic constraints are placed on the system to ensure that infeasible reactions are eliminated or, b) the value of λ is measured experimentally and the model is constrained accordingly.

Figure 2. Yeast growth and ^{14}C Incorporation. **A**, Yeast semi-log plot of growth during the experimental time course. **B**, Intracellular amino acid concentrations for glutamate family amino acids. **C**, Intracellular amino acid concentrations for non-glutamate family amino acids **D,** Total cellular incorporation of ^{14}C label. **E**, Incorporation of ^{14}C label in the intracellular polar metabolite pool. Mean values for three independent replicates are plotted with error bars showing standard error of the means.

Figure 3. Constraint of iND750 flux model with external metabolic fluxes. **A**, Media glutamate family amino acid concentrations during the time course of the experiments. **B,** Media non-glutamate family amino acid concentrations during the time course of the experiments. Mean values for three independent replicates are plotted with error bars showing standard error of the means. **C**, Yeast metabolic flux variability constraints generated by incorporation of amino acid consumption rates into the FBA model. DERN = system constraint using consumption rates of aspartic acid, glutamic acid, arginine, and asparagine. All = system constraint using consumption rates of all measured amino acids.

Figure 4. Measurement of intracellular metabolic fluxes. **A**, The pathway of Gln uptake, conversion to Glu, and GSH synthesis in yeast. **B**, ^{14}C label incorporation from ^{14}C Glu into Glu and GSH normalized to cell number. **C**, ^{14}C label incorporation from ^{14}C Glu into Glu and GSH normalized to intracellular concentrations of the respective metabolites. Metabolic fluxes can be calculated directly from the rate of ^{14}C incorporation into Glu and GSH. Mean values for three independent replicates are plotted with error bars showing standard error of the means.